Experiments on the relative mobility of mudflow as submarine slide simulation using lock-exchange system

Zainul Faizien Haza
Civil Engineering Department
Universiti Teknologi PETRONAS
Bandar Seri Iskandar, Perak, Malaysia
Email: zainulfaiz@gmail.com

Indra Sati H Harahap
Civil Engineering Department
Universiti Teknologi PETRONAS
Bandar Seri Iskandar, Perak, Malaysia
Email: indrasati@petronas.com.my

Abstract— **This paper has intention to inspect the behavior of gravity flows moving on beds in order to simulate the phenomenon of submarine slide. This objective is implemented by performing laboratory experiment using rectangular glass channel. The full-depth lock-exchange system and an image analysis technique are applied to measure the distance-time advancement of the gravity flows formation. A two-chamber material of mud and water is used to generate gravity flows. The model takes into account the kaolin clay content percentage of mud and the mixing region due to interaction between mud and water. Several tests are run to calibrate an entrainment parameter in order to reproduce gravity currents moving on sloping beds. The comparison between numerical and experimental results shows that the developed model is a valid tool to reproduce gravity current's dynamics.**

Keywords-gravity flow; submarine slide; lock-exchange system; mudflow

I. INTRODUCTION

Submarine landslides have denotation of failures within the sloping seafloor that cause the displacement of seabed sediments. It represents the predominant processes of sediment transport from shallow water shelf into deep seabed. It has become a serious and complex problem in the marine field. This is because submarine slide causes damage to the seabed environment in general and to the seabed facility constructed by humans as a means of sea-based activities in the field of business, industry, and maintenance of the environment itself. In this context that submarine slides are considered as one of geo hazard problems. These submarine slide geo hazard include slope instability, mud volcanoes and mudflows, gas hydrates, fluid seepage, bottom currents, and boulders.

According to sediment transport movement, the most involved material in this event was mud or slurry. It can be seen at seabed sediment classification proposed by Folk [1], the triangular scheme was dominated by mud. In addition, Locat et al. [2] mentioned that submarine slides have several differences of mass movement content. This research has proposed a quadratics scheme of mass movement related to submarine slide.

Several experiment models have been conducted in order to investigate this phenomenon of submarine slide. In general, most of laboratory experiments simulated the debris flow in ambient water. In year 1999, Mohrig et al. [3] performed a laboratory simulation on mobility of muddy sub aqueous and sub aerial debris flows using a mixture of materials consisting of water, kaolin, silt and sand in certain percentage. Other experiment that in pertaining to the frontal dynamics of submarine debris flow was performed by Ilstad et al. [4] in year 2004. Laboratory experiment also used to estimate the impact forces exerted by a submarine debris flow on a pipeline. It was conducted by Zakeri et al. [5] in year 2008.

By referring to Folk's sediment scheme [1], it can be inferred that the most vulnerable material to slide is mud, clay rich material with high water content. For all that, at recent time, the basic behavior of sub aqueous mudflow has not particularly informed yet. Hence, this study is willing to investigate the basic characteristic of mudflow in water ambient related to movement aspect as structures formation, velocity, and run-out distance.

II. PROBLEM FORMULATION

Depending on the type of mixture (one or two phases) of mud sediment referred to Locat et al. scheme, its behavior will be best analyzed by fluid mechanics. This means, that for mudflows, where the rate of movement is fast so that there is no time for excess pore water dissipation, the mechanics of the movement cannot be adequately explained by soil mechanics but rather we must apply fluid mechanics principles [2].

Gravity flow is type of stratified fluids phenomena, happens when a denser fluid body intrudes into a less dense body of fluid [6]. In this study, gravity flow approach is adopted to discover the mudflow behavior.

One of appropriate systems that can be used to generate gravity flow is called lock-exchange system. This system is commonly used in which the initial kinematics viscosity and

978-1-4577-1884-7/11/$26.00 ©2011 IEEE

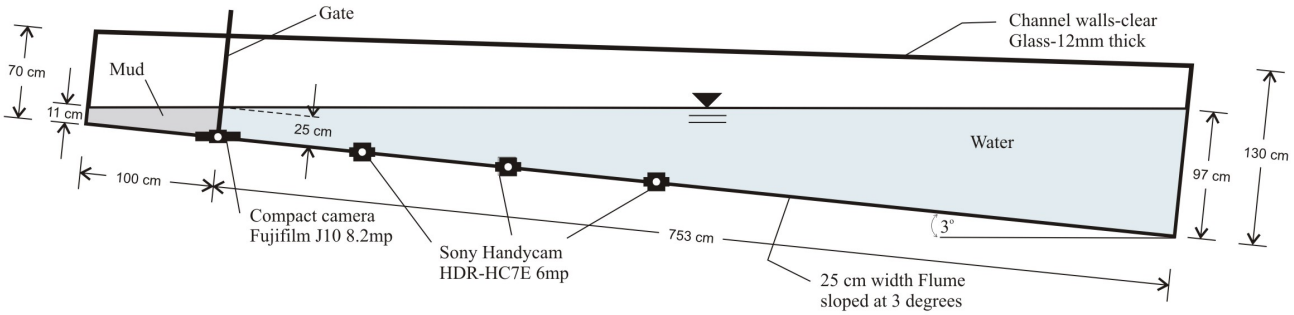

Figure 1. Schematic laboratory experiment of lock-exchange system

aspect ratio of currents were varied [7]. In this work, it is implemented by setting the laboratory equipments as shown in Fig. 1. After pulling the gate up, mud (slurry) forms an underflow spreading along the channel base.

Rheological test are described using Herschel–Bulkley model. The linear viscoplastic Bingham model was the most commonly used to describe rheology of debris or mudflow, but the Herschel–Bulkley model has been found to be more appropriate for describing the nonlinear viscoplastic behavior of debris flows [8-10].

$$(\tau - \tau_c) = K \cdot \dot{\gamma}^n \tag{1}$$

where, τ_c is the yield strength, K is equivalent to the dynamic viscosity, and $\dot{\gamma}$ the shear rate. The apparent viscosity, μ_{app}, is described by dividing the shear stress by the strain rate [11], thus

$$\mu_{app} = \frac{\tau_c}{\dot{\gamma}} + K \cdot \dot{\gamma}^{n-1} \tag{2}$$

In the experiment, the Boussinesq approximation may be applied regarding initial density ratios (ρ_i) in order to check the affection of density variations towards inertia. According to Amy et al. [7], initial density ratio was formulated as follow.

$$\rho_i = \sqrt{\frac{(\rho_f - \rho_w)}{(\rho_f + \rho_w)}} \tag{3}$$

where, ρ_f is density of slurry and ρ_w is water density.

Referring to the density rate involved in Eq. (1) and apparent viscosity defined by Eq. (2), the Reynolds number form is proposed as the following relationship,

$$\mathrm{Re}\, non-Newtonian = \frac{\rho \cdot U_\infty^2}{\mu_{app} \cdot \dot{\gamma}} = \frac{\rho \cdot U_\infty^2}{\tau} \tag{4}$$

where, U_∞ is the fluid velocity.

Observation was made by referring to gravity flow concepts that explain the phenomena of stratified fluids when a denser fluid body spreads under a less dense body of fluid [6]. In this case, slurry was the denser fluid that spreads under the water. Furthermore, Mok et al. provided the advance sketch of the typical gravity current front as shown in Fig 2.

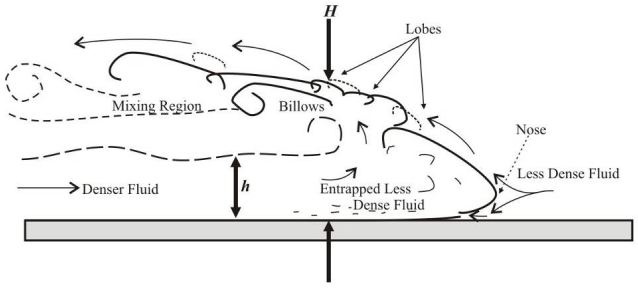

Figure 2. Sketch of a typical gravity current front (after [6])

In order to pursue more detail information about the behavior of slurry based on the velocity of movement, the magnitudes of the densimetric Froude number are then elaborated. The densimetric Froude number was defined as follows [3, 12].

$$Fr_d = \frac{v}{\sqrt{\left(\frac{\rho_f}{\rho_w} - 1\right) gD\cos\theta}} \tag{5}$$

where g is the acceleration due to gravity, D is the average thickness of debris and θ is the slope angle of the channel bottom, whereas ρ_f and ρ_w are referring to (3).

According to the Froude number and velocity correlation, De Blasio et al. [13] revealed a term of critical velocity V_{crit} formulated as,

$$V_{crit} \approx Fr_{crit}\left[\frac{g\cos\theta(\rho_f - \rho_w)D}{\rho_w}\right]^{1/2} \tag{6}$$

III. EXPERIMENTAL DESIGN

Experiment was performed in a rectangular channel of 8.53 m length, 0.25 width, and height of 0.7 m and 1.30 m at beginning and end respectively. Overall, channel was made of clear glass, including the base. Its has a adjustable horizontal position for setting the sloping base purpose. The base declivity was obtained by lifting the beginning edge of channel until reaching the expected slope. Figure 2 shows the laboratory test equipment. In this experiment, the slope angle used was 3°, referring to Hance [14] that the highest frequency density distribution of the average angle of the slope at failure for the seafloor slope failures was 3° to 4°.

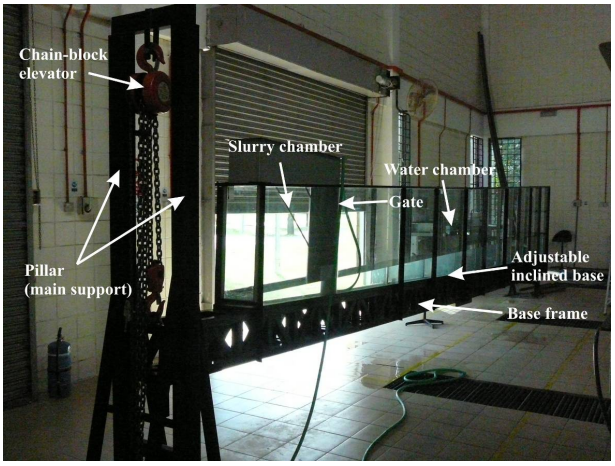

Figure 3. Laboratory test equipment

The basis of the experiment is simulating a lump of mud (i.e. slurry) sliding into a pool of water then flows over the surface of channel base. Fig. 1 shows the scheme of the experiment setup using a rectangular channel. The rectangular channel was divided into two main parts; namely, the slurry and the water, the two are separated by a vertical barrier (hereinafter referred to gate). The slurry has density of ρ_f whereas water has density of ρ_w, where $\rho_f > \rho_w$. The section of 1 m along the base from sidewall until the gate was occupied by the slurry, and then the water occupied the remaining section from gate until the end. The gate was removable. It was pulled upward rapidly until leaving the channel to let the slurry start flowing into the water.

IV. RESULT AND DISCUSSION

The slurries that made from mixture of refined kaolin and water in certain percentage were tested for its rheological properties, using *Brookfield Digital Viscometer DV-I+* equipment to determine the magnitude of the apparent viscosity, μ_{app}. All the results of the rheological experiments were repeated within ± 5% of clay content. Magnitude of density was tested also based on percentage of clay content using equipment of *Fann Four Scale Mud Balance.*

Results of rheological test are modeled using Herschel-Bulkley rheological model in (1) and are plotted in graph as shown in Fig.3.

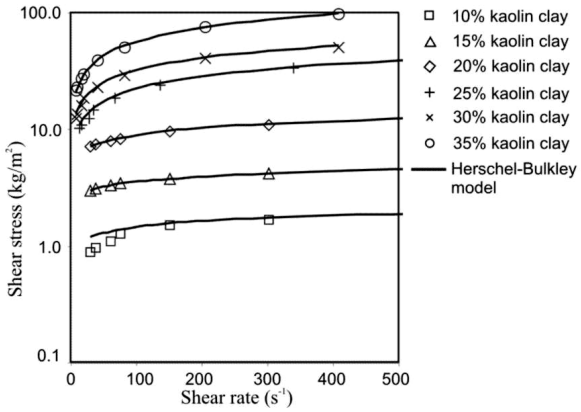

Figure 4. Slurry rheological test and Herschel-Bulkley model fits.

A dataset of rheological properties test in Table 1 represents the propagation of viscosity and density magnitudes among material models referred to kaolin clay percentage. Fann Mud Balance results values of slurry densities in range of 1054.8 kg/m^3 to 1266 kg/m^3.It can be inferred that both of viscosity and density magnitude are increasing due to increment of kaolin clay content.

TABLE I. PERCENTAGE CLAY CONTENT AND RHEOLOGICAL PROPERTIES

Kaolin clay percentage (%)	Density (ρ)		GS	Herschel-Bulkley rheological model
	(lbs/gal)	(kg/m^3)		
10	8.79	1054	1.07	$\tau = 0.6 + 0.2 \cdot \dot{\gamma}^{0.3}$
15	9.1	1092	1.1	$\tau = 2 + 0.4 \cdot \dot{\gamma}^{0.3}$
20	9.45	1134	1.13	$\tau = 3.4 + 1.3 \cdot \dot{\gamma}^{0.32}$
25	9.6	1152	1.2	$\tau = 2.1 + 3.2 \cdot \dot{\gamma}^{0.4}$
30	10.3	1236	1.23	$\tau = 5.7 + 3.7 \cdot \dot{\gamma}^{0.42}$
35	10.55	1266	1.27	$\tau = 9 + 4.7 \cdot \dot{\gamma}^{0.5}$

Referring to Table. 1 and (3), the slurry used for this experiment has value of ρ_i in range 0.17 to 0.27 for kaolin clay content below 25%, whereas 30% and 35% have value of 0.33 and 0.34 respectively.

Furthermore, Amy et al. obtained result of initial density ratios for all currents those vary between 0.1 and 0.35 [7]. The Boussinesq approximation, regarding variations in density that may be neglected as far as they affect inertia, is valid for lock exchange flows with $\rho_i < 0.3$. That flows became increasingly non-Boussinesq as ρ_i value increasing up to 1. Thus 30% and 35% kaolin clay content in this experiment were non-Boussinesq ($\rho_i > 0.3$), so it is inferred that density variations must be considered as factor that gives effect to mass movement characteristic.

In laboratory experiments, slurries were kept to have equal properties with the rheological test. Flow observation was limited at distance between gate to a point of 3.5 m.

Identification is including velocity, the shape of mass flow during slide, and run-out distance.

The total of 12 experiments addressed a typical slurry head velocity behavior. After gate opening, slurries velocity increased rapidly until a distance approximately of 0.5 m. It is considered as high potential energy affection due to position of deposit mass on top of slope. All experiments have similar behavior within this distance.

At distance point from 0.5 m to 3.5 m, slurry head velocities have range between about 0.15 m/s to 0.43 m/s. All percentage kaolin content have curve with trend of increasing velocity at distance of 3.5 m, except 30% and 35%. In experiment, 30% kaolin content stopped flowing at 4.2 m, whereas 35% at 2.3 m. The lower percentage was still flowing until the end of channel.

Fig.3 shows the image capturing of the shape similarities at the distance point of 2.5 m. Flowing mass of 35% clay could not be captured due to its stop flowing at distance of 2.3 m. The arrowhead of flowing mass inferred the percentage of clay. It was increasingly sharp due to higher viscosity and density.

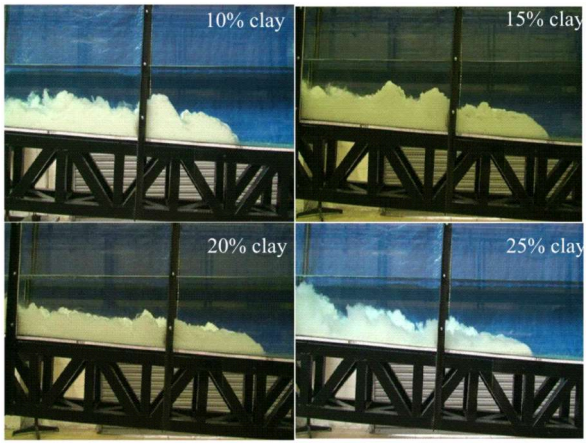

Figure 5. Image capturing at distance of 2.5 m

The body shape of slurry during flowing was in conformity with sketch of typical gravity current proposed by Mok et al. (see Fig. 2.). Slurry flow performed lobes, billows and mixing region as well as dense fluid intruded into less dense fluid. Various percentage of kaolin clay content addressed a significant difference of head formation; higher percentage formed the thinner head (i.e. decreased value of H).

With reference to recorded movement data, the head velocities were figured as graph of function of time versus run-out distance. The graph of velocities is made by determining the distance along the slope with interval of 0.25 m, then dividing those intervals with measured of the time that is used by the leading edge of slurries body to reach intervals in a sequence. Fig. 6. shows the propagation of head velocity during flow, starting from gate point until distance of 3.5 m.

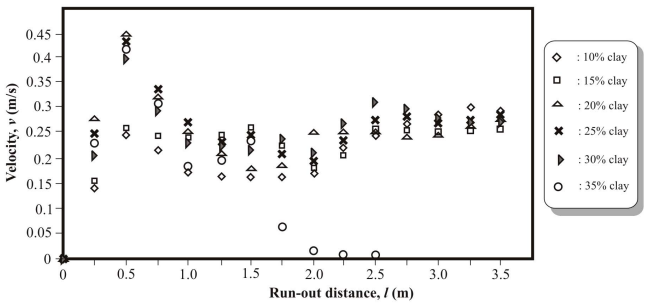

Figure 6. Head velocities at distance range of 0 to 3.5 m

Similar to a laboratory experiment, numerical modeling was also pointed observations of the result to correlation between mass properties and velocities. It could be figured in graph as shown in Fig.6. According to fit line profile, it displays that flow behavior of slurry simulated by CFD, was tending to flow similarly to which performed on laboratory experiments.

Observation was started at t = 0 s and l = 0 m; it was the moment when the gate was removed and the point where slurry allowed to start moving out from its compartment. Acquisition data as movement recording was limited until l = 3.5 m, but its time was not limited. This process was stopped when the nose (i.e. the leading edge) of slurry flow body reached distance point of 3.5 m. By referring to Fig. 6, it could be seen that immediately after the gate was opened, the slurry flow was performing acceleration until distance point of about 0.5 m. The rapid increasing of head velocity was appropriately caused by potential energy of slurry mass, according to level difference formed by sloping base.

Further observation, the flows are traced by plotting graph of time, t versus run-out distance, l.

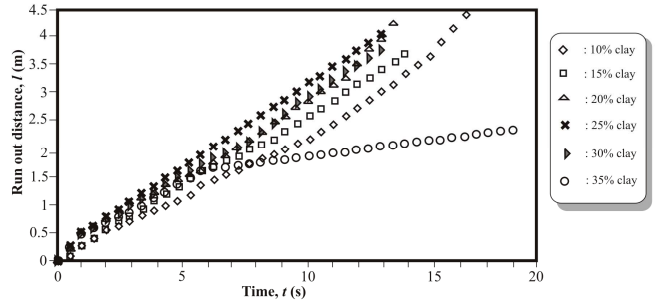

Figure 7. Run-out distance of slurry flow referred to elapsed time

Initial step to determine the value of Froude number and Reynolds number is measuring the average thickness of slurry during sliding from gate until distance of 2.5 m. Fig. 8 show the sketch of flowing slurry shape including its thickness measurements.

The average thickness D is obtained by plotting sketch of slurry into graph of 0.05 m interval (see Figure 7.a.) and then measuring the average of thickness vertically. This method has result that the value of D as shown in Table 2.

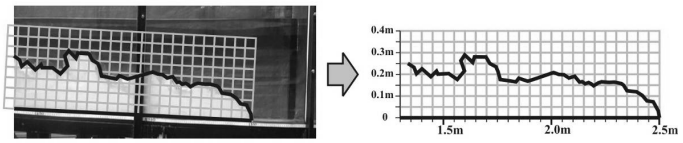

(a)

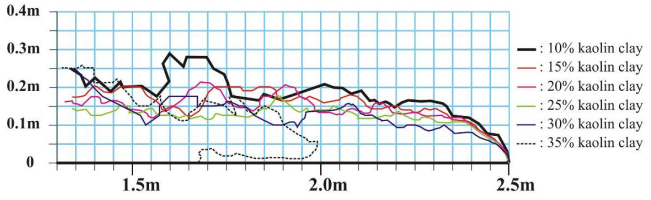

(b)

Figure 8. (a) Example of sketching the shape of slurry for 10% kaolin clay content; (b) Compilation shape sketch all kaolin clay percentage.

Based on these values of D, Froude number is calculated using magnitude of velocities at distance of 2.5 m.

TABLE II. AVERAGE THICKNESS OF SLURRY AND FROUDE NUMBER

Kaolin clay content (%)	**10**	**15**	**20**	**25**	**30**	**35**
Average thickness (D) (m)	0.182	0.161	0.149	0.134	0.133	-
Froude number (Fr_d)	0.239	0.202	0.181	0.180	0.208	-

Several research have been used the Froude number as a reference to observe the occurrence of hydroplaning, the conditions when a thin film of fluid is trapped between the bottom of the slide and the underlying ground. This film of fluid acts as a lubricant and reduces the resistance between those two surfaces [15]. Hydroplaning observation has been done through laboratory experiment and found that hydroplaning begins when Froude number approaches a critical value around 0.3, and hereinafter referred as Fr_{crit} [13, 16].

According to Table 3. in this experiment, Froude number has range of 0.180 to 0.239. Values of the critical velocity have range between 0.095 m/s to 0.167 m/s. Furthermore, previous estimation of the critical velocity (using Fr_{crit} = 0.3) gave values between about 0.3 m/s and 0.6 m/s for heights between 0.05 m and 0.2 m characteristic of the lab scale [13]. By referring to Froude number calculation in Table 2. and values of critical velocity, it can be inferred that hydroplaning did not occur in these experiments.

V. NUMERICAL APPROACH

This section deals with a brief description of the numerical model approach to complement the observation data of laboratory experiments. Numerical approach can be considered as a back calculation from laboratory experiments, because the input data was the same data applied in laboratory experiments. The rheology model used was the Herschel-Bulkley model as shown in Fig 4.

FLUENT, a state of the art CFD package, was totally used in this work to simulate the submarine slide model. This software was widely used in both industry and academia regarding flow and fluid movement. Input data were density and viscosity, which can be adopted from material properties test results as displayed in Table 1.

Simulation domain was established by a set of rectangular channel (refer to Fig. 1.). The boundary conditions were set as wall for left sideline and inclined base, and then for the top and right side line are set as pressure outlet. The continuum entity of fluid was set as boundary conditions to both slurry and water area. The material properties for each area were defined in FLUENT step referring to Table 2.

Volume of Fluid (VOF) method was selected as multiphase model. According to this model, 'segregated' solver was used. The setup was including first order implicit unsteady formulation and absolute velocity formulation with cell based gradient option. Since VOF method was selected, parameters are set as Geo-Reconstruct scheme with courant number of 0.25, then considered as open channel flow.

In the solution controls, an under-relaxation factor of pressure value was 0.3. Then multi grid controlled the termination restriction of 0.001 for pressure. For solution initialization, all initial values of gauge pressure, x-velocity, y-velocity and volume fraction of slurry were equal to zero. Integral forms of the momentum and continuity equations are solved sequentially. Several iterations over the solution cycle must take place to provide convergence at each time step since momentum and continuity equations are naturally coupled.

Iteration was set by 20 number of time steps with time step size of 0.001. The time stepping method was running iteration with maximum iterations per time step of 20. The convergence criterion for the continuity equation and the velocity components was selected as 0.001. The selected solver was segregated with absolute velocity formulation, unsteady, and cell based gradient option.

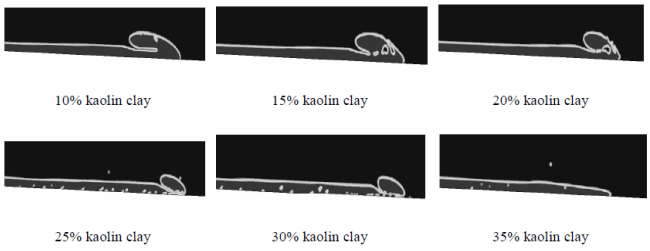

Figure 9. Image capturing in FLUENT simulation at distance of 2.5 m for all percentage kaolin clay content

For FLUENT simulation, 35% kaolin clay content stopped flowing at distance about 3.5 m. The shapes of slurry flow are different with with sketch of typical gravity current proposed by Mok as shown in Fig. 5 [6]. The slurry flow didn't generate lobes, billows and mixing region. Graph of velocities in FLUENT simulation is also made by using the same method as it is done for laboratory result. Fig. 10. shows the propagation of head slurry velocities.

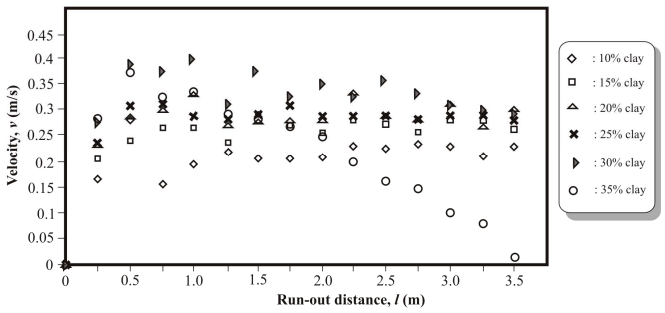

Figure 10. The slurry velocities in FLUENT simulation

Similar to laboratory work, further observation are performed on the flows by plotting graph of time, t versus run-out distance, l.

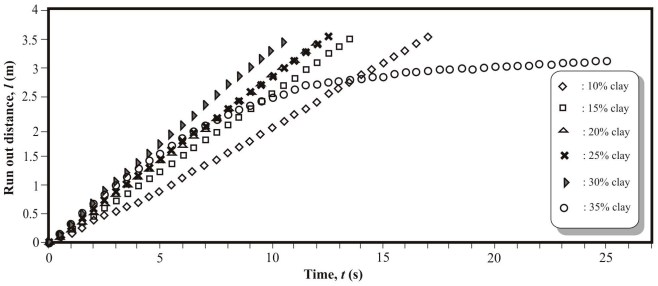

Figure 11. Run-out distance of slurry flow referred to elapsed time in FLUENT simulation

By comparing graph of slurry velocities in Fig. 9 to laboratory result (see Fig. 6.), there are similarities as follows;

- the slurry flow was performing rapid acceleration within distance of about 0.5 m to 1 m which it is caused by potential energy of slurry mass, according to level difference formed by sloping base.
- slurry with kaolin clay content of 30% has a tendency of continuous deceleration, even for 35% stopped flowing at a distance of 3.5 m according to its velocity which is deemed as zero at that point position.

Numerical simulation generated images in accordance with Fig 4 those show the entrapped less dense fluid during flow, in 25%, 30% and 35% particularly, but it was not able to display images of lobes, billows, and mixing region clearly.

The initial density ratios (ρ_i) equation is applied to elaborate the characteristic flow of 30% and 35% kaolin clay content. As calculated using (3) that both were non-Boussinesq ($\rho_i > 0.3$), it can be inferred that inertia affection were occurred in those flows. It is indicated by graph of velocity deceleration shown in either laboratory or numerical results.

VI. CONCLUSION

The slurry flow subsequently undergoes energy change from potential energy (E_p) due to kinetic energy (E_k) in moving stage. Referring to Fig. 7 and Fig. 11, it shows that E_p was affecting flowing range about 0.5 m to 1.0 m of run-out distance. After passing that distance, the flow will be related to E_k due to velocity. Based on the Boussinesq approximation, the slurry model has initial ratio density, ρ_i in range of 0.17 to 0.34. By these magnitudes, both critical velocity, V_{crit} and critical densimetric Froud number, Fr_{crit}, proposed by De Blasio et al.[6], are not achieved. Thus, it can be inferred that hydroplaning phenomena is not occurred in this experiment.

There was disagreement in mass flow formation between FLUENT and laboratory experiment. This perhaps due to the imperfect initial condition and some physical effects those were not numerically modeled.

In general, two methods of laboratory and numerical have conformity each other in submarine slide simulation using gravity flow approach with lock-exchange system. Even though, further research is needed to elaborate more engineering aspects related to laboratory equipments and features of the software.

REFERENCES

[1] R. L. Folk, "The Distinction between Grain Size and Mineral Composition in Sedimentary-Rock Nomenclature," *Journal of Geology,* vol. 62, pp. 344-359, 1954.

[2] J. Locat and H. J. Lee, "Submarine Landslides: Advances and Challenges," presented at the The 8th International Symposium on Landslides, Cardiff, U.K, 2000.

[3] D. Mohrig, *et al.*, "Experiments on the relative mobility of muddy subaqueous and subaerial debris flows, and their capacity to remobilize antecedent deposits," *Marine Geology,* vol. 154, pp. 117-129, 1999.

[4] T. Ilstad, *et al.*, "On the frontal dynamics and morphology of submarine debris flows," *Marine Geology* vol. 213 pp. 481-497, 2004.

[5] A. Zakeri, *et al.*, "Submarine debris flow impact on pipelines — Part I: Experimental investigation," *Coastal Engineering,* vol. 55, pp. 1209 - 1218, 2008.

[6] K. M. Mok, *et al.*, "Experimental Observations of The Flow Structures at Gravity Current Fronts," presented at the International Conference on Estuaries and Coasts, Hangzhou, China, 2003.

[7] L. A. Amy, *et al.*, "Abrupt transitions in gravity currents," *Journal of Geophysical Research,* vol. 110, pp. 1-19, 2005.

[8] J. Imran, *et al.*, "A numerical model of submarine debris flow with graphical user interface," *Computers & Geosciences,* vol. 27, pp. 717-729, 2001.

[9] S. Cohard and C. Ancey, "Experimental investigation of the spreading of viscoplastic fluids on inclined plane," *Journal of Non-Newtonian Fluid Mechanics,* vol. 158, pp. 73-84, 2009.

[10] N. J. Balmforth, *et al.*, "Shallow viscoplastic flow on an inclined plane," *Journal Fluid Mechanics,* vol. 470, pp. 1-29, 2002.

[11] A. Zakeri, *et al.*, "Submarine debris flow impact on pipelines — Part II: Numerical analysis," *Coastal Engineering,* vol. 56, pp. 1-10, 2009.

[12] S. G. Wright and H. Hu, "Risk Assessment for Submarine Slope Stability - Hydroplaning," Minerals Management Service, Austin, US, Final Project Report 1435-01-04-CA-35515, February 2007.

[13] F. V. D. Blasio, *et al.*, "Hydroplaning and submarine debris flows," *Journal of Geophysical Research,* vol. 109, pp. 1-15, 2004.

[14] J. J. Hance, "Development of a Database and Assessment of Seafloor Slope Stability based on Published Literature," Master of Science in Engineering, Faculty of the Graduate School, The University of Texas, Austin, 2003.

[15] H. Hu, *et al.*, "Hydroplaning of Submarine Slides and the Influence of Hydrodynamic Stresses," presented at the International Offshore and Polar Engineering Conference, San Francisco, California, 2006.

[16] D. Mohrig, *et al.*, "Hydroplaning of subaqueous debris flows," *Geological Society of America,* vol. 110, pp. 387-394, 1998.